Pathol. Oncol. Res. (2015) 21:357–366
DOI 10.1007/s12253-014-9828-0

RESEARCH

Emerin Expression in Well Differentiated Epithelial Lesions of Thyroid: Implications in Papillary Thyroid Carcinoma Diagnosis and Predicting Malignant Behavior

Ipek Coban · Asli Cakir · Tuba Dilay Kokenek Unal · Nuray Bassullu · Vildan Karpuz · Gulen Bulbul Dogusoy · Murat Alper

Received: 31 August 2013 / Accepted: 29 July 2014 / Published online: 14 August 2014

Abstract Recently, it has been reported that identifying nuclear membrane irregularities with anti-emerin antibody is useful for papillary thyroid carcinoma diagnosis. However, literature regarding the significance of emerin immunohistochemistry in thyroid is limited. We evaluated the diagnostic accuracy of the well-established nuclear alterations, nuclear protrusions and recently described nuclear shapes (garlands and star-like shapes) with emerin immunohistochemistry and hematoxylin- eosin stain in thyroid lesions. We further evaluated the diagnostic accuracy measures of tissue microarrays evaluated with both stains, to detect whether emerin immunohistochemistry improves the diagnostic accuracy for papillary thyroid carcinoma. For papillary thyroid carcinoma, pseudo- inclusions were best performers with emerin (diagnostic accuracy: 0.91), whereas with hematoxylin- eosin diagnostic accuracy of grooves was the highest (0.92). For follicular variant of papillary thyroid carcinoma, with both stains, predominately oval nuclear shape had the best diagnostic performance (diagnostic accuracy: 0.95). Nuclear protrusions were poor identifiers for papillary thyroid carcinoma. However, with emerin immunohistochemistry, they could successfully identify malignancy in 83 % of the cases. Using emerin immunohistochemistry, in addition to hematoxylin- eosin improved the diagnostic accuracy for papillary thyroid carcinoma when compared to hematoxylin- eosin evaluation only (sensitivity: 0.70 vs 0.86, negative predictive value: 0.81 vs. 0.94, diagnostic accuracy: 0.87 vs. 0.94). Consistent with the previous literature, our findings indicate that emerin immunohistochemistry may be used as an adjunct diagnostic method to identify papillary thyroid carcinoma. Additionally, we suggest that nuclear protrusions detected with emerin imunohistochemistry may be used as indicators of malignant behavior in small tissue samples of thyroid.

Keywords Emerin · Thyroid · Nucleus · Membrane

G. B. Dogusoy
Department of Pathology, Istanbul Bilim University School of Medicine–Florence Nightingale Hospitals, Istanbul, Turkey

A. Cakir
Department of Pathology, Medipol University School of Medicine, Istanbul, Turkey

T. D. K. Unal · M. Alper
Department of Pathology, Diskapi Yildirim Beyazit Training and Research Hospital, Ankara, Turkey

I. Coban (✉)
Department of Pathology and Laboratory Medicine, Istanbul Bilim University, School of Medicine, Cemil Aslan Guder Sok. No: 8 Gayrettepe, İstanbul 30342, Turkey
e-mail: ipekco@gmail.com

I. Coban
e-mail: ipek.coban@florence.com.tr

I. Coban · N. Bassullu · V. Karpuz
Department of Pathology, Istanbul Bilim University, School of Medicine, Istanbul, Turkey

Introduction

Hematoxylin- eosin (HE) stain is considered to be the gold standard of diagnosis in thyroid pathology. Among these, diagnosing papillary thyroid carcinoma (PTC), especially follicular variant (FV) of PTC and predicting malignant behavior in non-PTC follicular neoplasia (FN) have been the two most contentious areas in thyroid pathology.

Nuclear criteria are well established for PTC but the inter-observer variability results are by no means perfect [1–3]. This may partly be attributed to the threshold differences among experts in applying the extend and degree of these nuclear criteria to the diagnosis [2]. However, it has been suggested that at least in some of the cases especially in FV of PTC, where

pathologists are obligated to rely on nuclear morphology, indirect visualization of the nuclear membrane by conventional HE staining may contribute to underdiagnosing some of the cases [4]. Furthermore, artificial nuclear findings may cause over diagnosis in small tissue samples. Several immunohistochemical markers such as Hector Battifora mesothelial antigen-1 (HBME-1), Cytokeratin 19 (CK 19), and galectin-3 (Gal3) have been mentioned and molecular studies have been conducted but the results could not add much on daily practice [5–12].

In terms of non-PTC FN, it has been indicated that malignant non-PTC FN is being diagnosed less frequently [13]. A trend toward over diagnosing non-PTC FN as FV of PTC [14], in addition to improvements in early detection of FN by imaging techniques may contribute in this ascertainment. An attempt to differentiate non-PTC FN and FV of PTC may be challenging due to the limitations of the methods used as discussed above.

Emerin is an inner nuclear membrane protein which has important interactions with the cytoskeleton and related proteins [15, 16]. Recent studies have indicated that, even though emerin protein expression is not related to the underlying pathogenetic mechanisms in PTC [17], emerin immunohistochemistry(IHC) provides an enhanced view of the nuclear envelope and tracing the nuclear alterations with anti- emerin antibody may be a useful diagnostic tool for thyroid lesions [4, 18–20]. In addition, with emerin IHC new nuclear alterations, such as *garlands* [4] *and star- like* nuclear shapes [18] have been described.

Given the observations that highlighting nuclear membrane morphology with emerin IHC may contribute to the diagnostic workup of PTC, we aimed to investigate whether nuclear alterations detected with this stain can serve as accurate criteria in the diagnostic workup of PTC. Additionally, we compared the diagnostic accuracy of HE stained TMA samples with HE and emerin stained samples to detect if using emerin IHC improves the diagnostic accuracy for PTC in these small tissue samples.

Materials and Methods

Case Selection

This study was approved by Diskapi YB Training and Research Hospital Ethics and Research Committee (Approval ID: 29/02.05.12.2011).

From the archives of the Pathology Department of Diskapi Y.B. Training and Research Hospital, cases with non- neoplastic and WD neoplastic epithelial thyroid lesions were identified through a retrospective review of surgical pathology reports signed out between the years of 2004–2010. A concensus session was performed by 3 pathologists (IC, TDKU, and AC) to detect cases with uniform agreement. HE stained slides were de-identified and reviewed. After a total of 340 cases including 44 diffuse hyperplasia (DH), 21 Hashimoto's thyroiditis (HT), 77 follicular adenoma (FA), 48 follicular carcinoma (FC), and 150 PTC (classical PTC, $n=52$ and FV of PTC, $n=98$), were selected for study purposes, the review was arrested.

Slides of the study cases were further evaluated by 3 pathologists (IC, TDKU, and AC) to detect the most representative areas for the nuclear changes and corresponding areas in the tissue blocks were used for constructing tissue microarray (TMA)s. Both HE staining and emerin IHC were completed on formalin fixed, paraffin embedded TMA sections for each case.

Emerin Immunohistochemistry

Methodology

Five micron sections of formalin-fixed, paraffin embedded TMAs were obtained. All slides were loaded onto an automated system (Leica Bond Max). Sections were deparaffinized and rehydrated with deionized water. Then, they were heated in citrate buffer, pH 6.0, for 20 min and exposed to 3 % hydrogen peroxide for 10 min. Sections were incubated with primary antibody (anti-emerin antibody, clone 4G5, diluted 1:10; Thermo Fisher Scientific Laboratories, Fremont, CA, USA) for 25 min, post primary 10 min, labeled polymer for 10 min, 3′3-diaminobenzidine chromogen for 10 min, and counterstained with hematoxylin for 13 min. These incubations were performed at 37 °C. Incubations with hydrogen peroxide, post primary, labeled polymer, chromogen and hematoxylin were performed with Bond Polymer Refine Detection ref # DS9800. Between incubations, sections were washed with tris-buffered saline (Bond Wash Solution 10X Concentrate Catalog no: AR9590). Cover slipping was performed. Normal thyroid tissues were used as positive controls and processed with other tissue sections.

Evaluation of TMA Slides

Emerin IHC and HE staining was completed on TMAs and slides were reviewed by a single pathologist (IC). Each slide was reviewed under ×400 magnification and when cells with evaluated parameters are recognized, they were examined under oil immersion magnification (×100 objective). Presence of previously well-established nuclear alterations and newly described nuclear criteria such as star-like shapes and garlands were investigated and additional findings were noted. Thus, a group of nuclear features listed in the summary text (Textbox 1) was compiled for examination. During evaluation of slides, areas with extensive nuclear overlap and obscured nuclear boundaries were avoided.

Textbox 1: Nuclear Alterations:

Nuclear invaginations (Fig. 1)

- Grooves: Narrow invaginations of nuclear envelope [4, 18, 20], (Fig. 1a).
- Pseudo-inclusions: Wide infoldings/pockets of nuclear membrane [4, 18, 20], (Fig. 1b).

Nuclear protrusions (NPs)

- Nuclear buds (NBs): Small protuberances of the nuclear envelope that have similar features to the micronuclei except that they are connected to the main nucleus with a narrow or wide stalk depending on the stage of the budding process [26, 27], (Fig. 2a–c).
- Micronuclei (MN): Regular nuclear fragments in the cytoplasm exhibiting the inclusion criteria listed below [26, 27], (Fig. 2d),
  - *A diameter smaller than 1/3 of the main nucleus*
  - *Round/oval shape with regular contours*
  - *Same staining intensity with the main nucleus*
  - *No connection to the main nucleus*

Changes in the nuclear shape

- Garlands: Circumferential minute curls along the nuclear membrane producing a garland-like effect [4], (Fig. 3a)
- Star- like: Multiple plicae or deep infoldings of the nuclear membrane building up a star shaped structure [18], (Fig. 3b).
- Crescents: Crescent shaped nuclei [20], (Fig. 3c).
- Predominately oval nuclear shape [20], (Fig. 3d)

Statistical Analysis

Data were analyzed initially by Chi-square test and Fisher's exact test as appropriate. Frequency of different nuclear changes detected with HE and emerin IHC was calculated. Nuclear alterations, whose recognition have improved with emerin IHC, were also noted. Diagnostic accuracy measures including sensitivity (true positives/true positives + false negatives), specificity (true negatives/true negatives + false positives), positive predictive value (PPV = true positives/true positives + false positives), negative predictive value (NPV = true negatives/true negatives + false negatives) and diagnostic accuracy (DA = true positives + true negatives/true positives + false positives + true negatives + false negatives) rates of each nuclear parameter for PTC and FV of PTC were calculated. Further evaluation was performed to determine if there is any significant difference in nuclear protrusion frequency between different diagnostic groups (neoplastic vs. non- neoplastic, benign vs. malignant, FA vs. FC). DA measures of nuclear protrusions in these diagnostic groups were also assessed by using the same statistical methods.

Finally, for PTC and FV of PTC (among FN), diagnostic accuracy of these small tissue samples with both stains and HE only were assessed. Reference diagnoses were the adjudicated concensus diagnoses of 3 reviewers (IC, TDKU, and AC). The 95 % confidence intervals for proportions based on a binomial probability distribution were also calculated to assess the accuracy of these estimates. $P<0.05$ was regarded as statistically significant.

Results

A total of 340 cases were examined. Of these, 65/340 (19 %) were non- neoplastic (DH = 44; HT $n=21$) and 275/340 (81 %) were neoplastic with 77/275 (28 %) being FA. Among 198 malignant cases, 48 (24 %) were FC and 150 (76 %) were PTC (classical PTC, $n=52$ and FV of PTC, $n=98$).

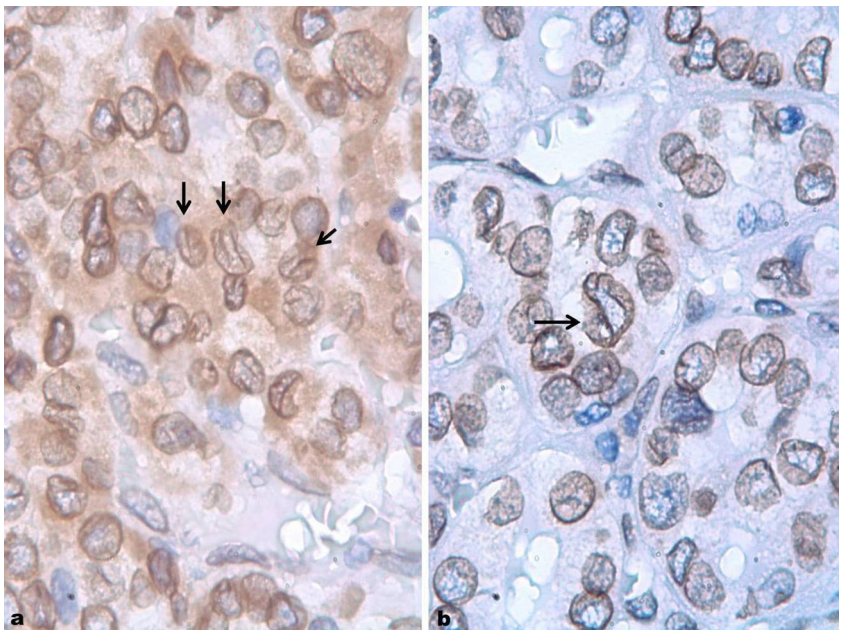

Fig. 1 Nuclear invaginations in PTC by emerin IHC. **a** Grooves appear as deep narrow invaginations of the nuclear membrane (*arrows*). **b** Nuclear pseudo-inclusions appear as wide invaginations of the nuclear membrane (*arrow*). Original magnifications: ×1,000 for **a** and **b**

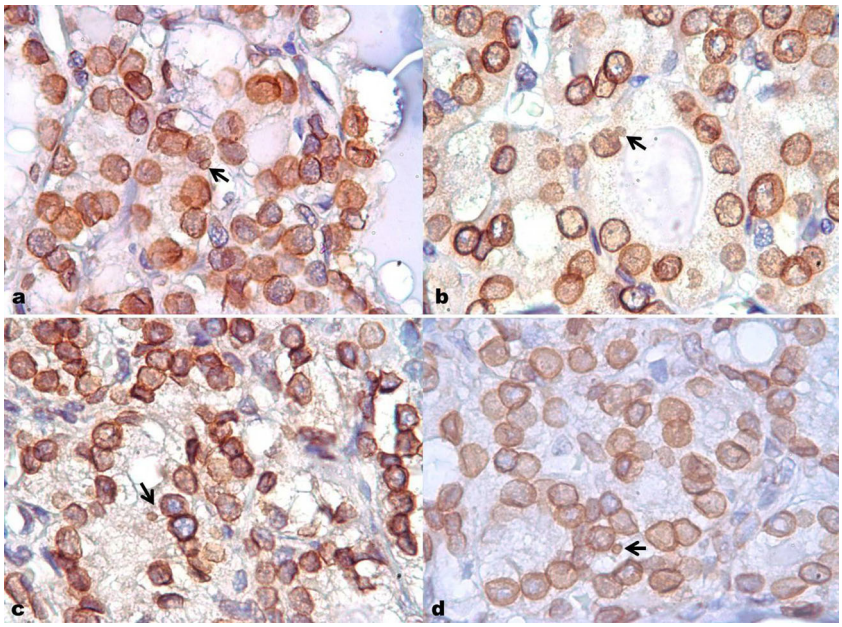

Fig. 2 NPs in PTC. **a** A NB in a case of PTC by emerin IHC is represented. It is regularly shaped and has the same intensity of staining with the main nucleus (*arrow*). **b** NB, attached to the main nucleus by a wide stalk (*arrow*). **c** A, barely visible, thin stalk is connecting the NB to the main nucleus (*arrow*). **d** MN with no connection to the main nucleus (*arrow*). Original magnifications: ×1,000 for **a**, **b**, **c** and **d**

Nuclear membrane alterations were easily identifiable with Emerin IHC (Fig. 4). Emerin was strongly expressed in the nuclear membrane of epithelial cells, whereas the nuclear membrane of stromal cells or inflammatory cells were negative or weakly positive (Fig. 5). Among all cases examined, the nuclear alteration, whose recognition was improved most with emerin IHC, was NPs (detected in 73 additional cases) followed by, pseudo-inclusions (n: 62 cases), crescents (n: 35 cases), star-like shapes (n: 33 cases), garlands (n: 20 cases) and grooves (n: 18 cases). No recognition improvement was observed in oval nuclear shape predominance.

Nuclear Features in PTC

In PTC, nuclear protrusions (NPs), pseudo-inclusions, grooves, garlands, crescents, star-like shapes and predominately oval nuclear shape were significantly more frequent, compared to non-PTC lesions ($p<0.0001$) (Table 1). All nuclear parameters but NPs were significantly more frequent in FV of PTC than non- PTC FN ($p<0.0001$). NPs were slightly more common in FV of PTC, but the difference between groups was not significant ($p=0.07$ for Emerin and 0.1 for HE) (Table 1).

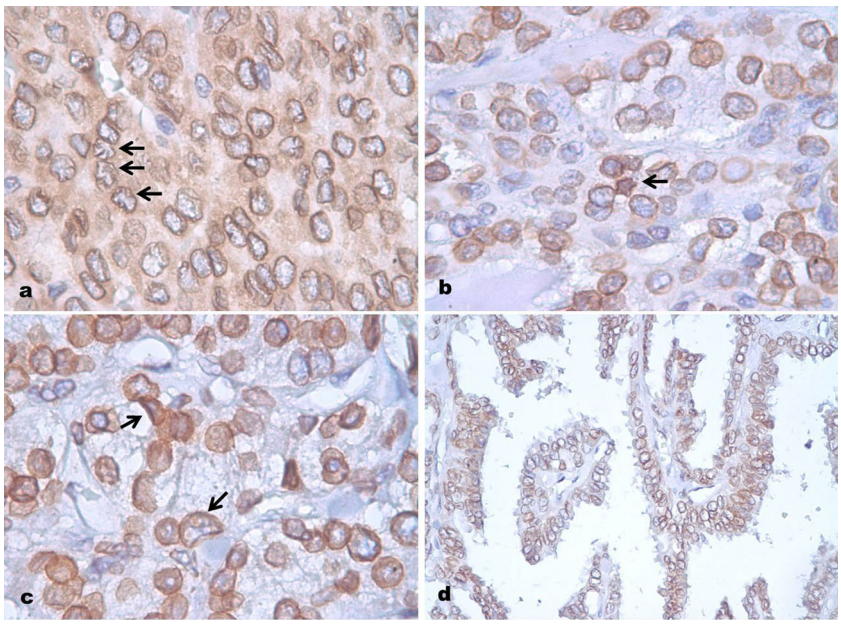

Fig. 3 Changes in the nuclear shape in PTC by emerin IHC. **a** Garlands (*arrows*). **b** Star- like nuclear shape (*arrow*). **c** Crescents (*arrows*). **d** Predominance of oval nuclear shape. Original magnifications: ×1,000 for **a**, **b** and **c**; ×200 for **d**

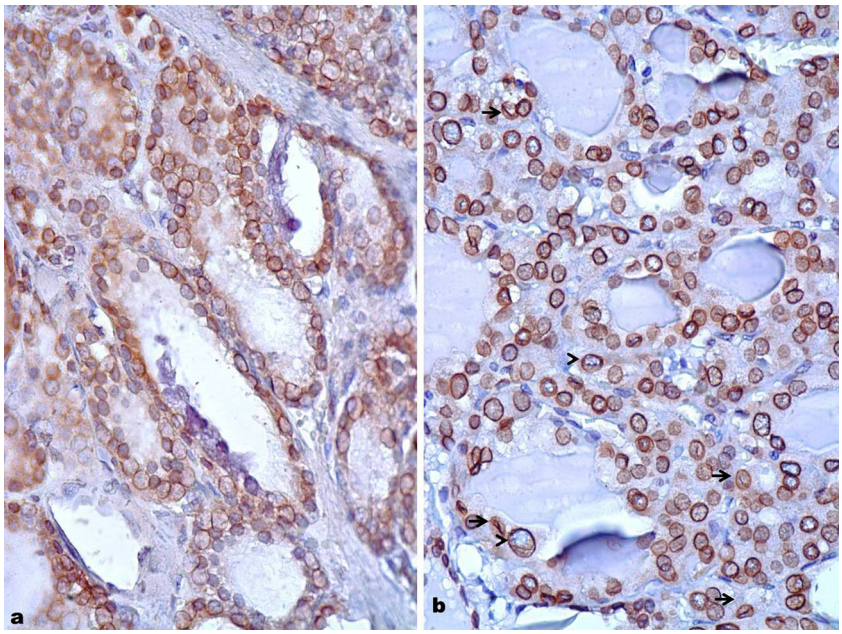

Fig. 4 **a** Emerin IHC in DH. Nuclei appear uniform with regular contours. **b** Widespread grooves (*arrowheads*), occasional inclusions (*arrows*) are easily discernable with emerin IHC in a case of FV of PTC. Original magnifications: ×400 for **a**, **b**

For identification of PTC among all lesions examined, with emerin IHC, pseudo-inclusions revealed the best diagnostic performance (sensitivity: 0.94; specificity: 0.88; PPV: 0.86; NPV: 0.95; DA: 0.91). Star- like shapes, garlands and crescents, predominately oval nuclear shape and grooves also had good diagnostic performances. When evaluated with HE, grooves had the best diagnostic performance (sensitivity: 1.00; specificity: 0.86; PPV: 0.84; NPV: 1.00; DA: 0.92). Whereas, although their specificity for PTC diagnosis was very high (0.99), overall performance of pseudo-inclusions for PTC diagnosis was fair (DA: 0.74). NPs were poor identifiers both when detected with emerin IHC (DA: 0.69) and HE (DA: 0.63) Diagnostic accuracy measures of all nuclear parameters for PTC are listed in Table 2.

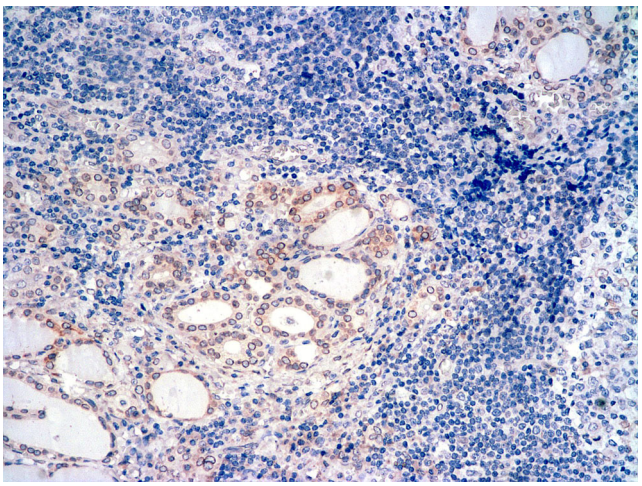

Fig. 5 Thyrocyte nuclei are diffusely positive for emerin. Whereas, stromal cells and inflammatory cells are negative. Original magnification: ×200

Oval nuclear predominance, both when detected with HE and emerin IHC, had the best diagnostic performance for FV of PTC among FN (sensitivity: 0.93; specificity: 0.97; PPV: 0.96; NPV: 0.95; DA: 0.95). Pseudo-inclusions, when detected with HE, performed poorly in identifying FV of PTC among FN (DA: 0.65). However, with emerin IHC, pseudo- inclusions could successfully identify these lesions (DA: 0.90). NPs failed to detect FV of PTC among FN (DA: 0.54) with emerin stain, and were poor performers with HE (DA: 0.60). Diagnostic accuracy measures of all nuclear parameters for FV of PTC among FN are listed in Table 3.

NPs in Different Diagnostic Groups

Both with HE and emerin IHC, NPs were significantly more frequent in neoplastic lesions than in non- neoplastic lesions ($p<0.0001$). Malignant lesions presented nuclear protrusions more commonly than benign lesions ($p<0.0001$). Furthermore, significant difference persisted when FC were compared with FA ($p<0.0001$). NPs showed good performance in identifying malignancy (DA: 0.82), when detected with emerin IHC. On the contrary, their diagnostic accuracy for malignancy was poor when detected with HE (DA: 0.63). Among non-PTC follicular neoplasia, NPs, with emerin IHC, could accurately detect 83 % of cases with malignant behavior (FC), whereas the diagnostic accuracy with HE was fair (74 %). Comparison of the frequencies of NPs between different diagnostic categories and their diagnostic accuracy measures are shown in Tables 4 and 5, respectively.

Table 1 Nuclear alterations detected with HE and emerin IHC (PTC compared with non- PTC lesions and FV of PTC compared with non-PTC FN)

Nuclear alterations	PTC (n: 150) vs. Non-PTC (n: 190); *p* value		FV of PTC (98 cases) vs. Non- PTC FN (n: 125); *p* value	
	Emerin	HE	Emerin	HE
NPs	117 (78 %) vs. 70 (37 %); <0.001	71 (47 %) vs. 43 (23 %); <0.001	65 (66 %) vs. 68 (54 %); 0.07	44 (45 %) vs. 43 (34 %); 0.1
Garland-like shape	121 (81 %) vs. 15 (8 %); <0.0001	100 (67 %) vs. 6 (3 %); <0.0001	82 (84 %) vs. 15 (12 %); <0.0001	74 (%76) vs. 6 (5 %); <0.0001
Pseudo-inclusions	107 (71 %) vs. 19 (15 %); <0.0001	64 (43 %) vs. 0 (0 %); <0.0001	55 (56 %) vs. 18 (14 %) <0.0001	20 (20 %) vs. 0 (0 %) <0.0001
Star-like shape	127 (85 %) vs. 24 (13 %); <0.0001	106 (71 %) vs. 12 (6 %); <0.0001	75 (77 %) vs. 20 (16 %); <0.0001	66 (67 %) vs. 12 (10 %)
Crescents	130 (87 %) vs. 21 (11 %); <0.0001	103 (69 %) vs. 13 (7 %); <0.0001	84 (86 %) vs. 18 (14 %); <0.0001	70 (88 %) vs. 28 (20 %); <0.0001
Predominately oval shape	112 (75 %) vs. 4 (2 %); <0.0001	112 (75 %) vs. 4 (2 %); <0.0001	67 (68 %) vs. 4 (3 %); <0.0001	67 (68 %) vs. 4 (3 %); <0.0001
Grooves	150 (100 %) vs. 45 (24 %); <0.0001	150 (100 %) vs. 27 (14 %); <0.0001	98 (100 %) vs. 32 (26 %); <0.0001	98 (100 %) vs. 22 (18 %); <0.0001

PTC papillary thyroid carcinoma, *FV* follicular variant, *FN* follicular neoplasia, *NPs* nuclear protrusions; $p<0.05$ is significant

Nuclear Features in Non- Neoplastic Thyroid Lesions

Grooves were the most frequent nuclear parameter in non-neoplastic lesions both when detected with HE (5/65, 8 %) and emerin IHC (13/65, 20 %). They were more commonly observed in HT than DH both with HE (2/21, 10 % vs. 2/44, 5 %) and emerin IHC (8/21, 38 % vs. 2/44, 5 %). Crescents and star-like shapes were only evident in HT. The frequency of crescents was the same both with HE and emerin IHC (3/21, 14 %). Whereas, star-like shapes were only evident with emerin IHC (2/21, 10 %). In HT no nuclear protrusion was observed with HE stain, although with emerin IHC, in 2 cases (2/21, 10 %) NPs were detected. Pseudo-inclusions, garlands and predominately oval nuclear shape were not observed in non- neoplastic lesions.

Previously described nuclear alterations related with chromatin content such as nuclear clearing or presence of nucleoli were not interpretable with emerin IHC as the stain only highlighted nuclear envelope and related structures such as NPs.

Diagnostic Efficacy of Emerin IHC for PTC

When all TMA samples were evaluated with HE only to identify PTC, diagnostic accuracy was good (0.87) and the sensitivity was fair (0.70). Further evaluation of tissues with emerin IHC, in addition to HE, improved the sensitivity (0.86), NPV (0.90) and DA (0.94), (Table 6)

For identification of FV of PTC among FN, diagnostic accuracy with HE only, was good (0.81) but sensitivity was poor (0.55). Additional evaluation of tissues with emerin IHC, improved sensitivity (0.79), NPV (0.86) and the DA (0.91), (Table 6).

Discussion

In an effort to better delineate its diagnostic utility, we examined emerin protein expression in a variety of WD non-neoplastic and neoplastic epithelial lesions.

As the distribution of the nuclear changes in benign and malignant thyroid lesions may not be uniform, especially in FV of PTC, the representative areas were carefully selected by acquiring the agreement of three pathologists to avoid/minimize the possible bias in data interpretation in TMAs, such as under- or over-representation of the nuclear changes of a given lesion.

Consistent with the previous observation of Asioli et al. [18], we observed that emerin highlights only the nuclear membrane of thyrocytes without the obscuring effect of the cytoplasm or stromal cells. This feature of emerin IHC, allows easy identification of nuclear membrane irregularities.

Pseudo-inclusions appeared as wide infoldings/pockets of nuclear membrane that presented as lighter staining areas and darker peripheral edges compared to the intensity of staining in the neighbouring nuclear membrane areas (Fig. 1b). As the stain only highlights the nuclear membrane of thyrocytes, common mimickers of pseudo-inclusions, such as nuclear bubbles due to processing artifacts [21], superimposed erythrocytes [20] could easily be avoided.

In our study, both with HE and emerin IHC, pseudo-inclusions were significantly more frequent in PTC (among all cases) and in FV of PTC (among FN). With emerin IHC, recognition of pseudo- inclusions was improved in 62 of 340 cases examined. On the contrary, in the study by Kinsella et al., although an improvement in the detection frequency of pseudo- inclusions were noted, no significant difference between the frequencies of pseudo-inclusions in PTC and

Table 2 Diagnostic accuracy measures of nuclear alterations detected with emerin IHC and HE in distinguishing PTC from non- PTC WD epithelial lesions of thyroid

Nuclear alterations	Emerin, (%) (95 % CI, %)					HE, (%) (95 % CI, %)				
	Sensitivity	Specificity	PPV	NPV	DA	Sensitivity	Specificity	PPV	NPV	DA
NPs	78 (70–83)	63 (56–70)	62 (55–90)	78 (71–84)	69 (65–74)	39 (31–47)	81 (75–86)	61 (51–71)	63 (56–69)	63 (54–66)
Garland-like shape	80 (74–86)	92 (87–95)	89 (82–93)	85 (80–90)	87 (83–90)	67 (59–74)	96 (93–99)	94 (88–98)	79 (73–84)	83 (77–87)
Pseudo-inclusions	94 (89–97)	88 (83–92)	86 (80–91)	95 (91–98)	91 (88–94)	43 (35–51)	99 (97–100)	99 (93–100)	69 (63–74)	74 (66–77)
Star-like shape	84 (78–90)	87 (81–91)	84 (77–89)	87 (74–85)	86 (79–87)	71 (63–77)	94 (89–96)	90 (83–94)	80 (74–85)	84 (51–100)
Crescents	86 (80–91)	88 (84–93)	86 (79–91)	89 (84–93)	87 (84–91)	67 (61–76)	93 (89–96)	89 (81–94)	79 (73–84)	82 (76–86)
Predominately oval shape	74 (67–81)	97 (95–99)	96 (91–99)	83 (77–87)	87 (83–90)	75 (67–81)	98 (95–99)	97 (91–99)	83 (77–88)	88 (82–91)
Grooves	100 (96–100)	76 (70–81)	76 (70–82)	100 (97–100)	86 (82–90)	100 (97–100)	86 (80–90)	84 (78–90)	100 (97–100)	92 (90–96)

PPV positive predictive value, *NPV* negative predictive value, *DA* diagnostic accuracy, *CI* confidence interval, *NPs* nuclear protrusions

Table 3 Diagnostic accuracy measures of nuclear features detected with HE stain and emerin IHC in distinguishing FV of PTC from non- PTC FN

Nuclear alterations	Emerin, (%) (95 % CI, %)					HE, (%) (95 % CI, %)				
	Sensitivity	Specificity	PPV	NPV	DA	Sensitivity	Specificity	PPV	NPV	DA
NPs	66 (56–75)	45 (37–54)	48 (41–57)	63 (53–73)	54 (48–61)	44 (35–54)	71 (63–78)	54 (54–669)	62 (54–70)	60 (6–100)
Garland-like shape	83 (75–90)	88 (81–93)	84 (76–90)	87 (80–92)	86 (80–90)	75 (66–83)	95 (90–98)	92 (84–97)	83 (76–89)	87 (59–100)
Pseudo-inclusions	100 (95–100)	83 (77–89)	82 (74–88)	100 (96–100)	90 (86–94)	20 (14–30)	100 (96–100)	100 (80–100)	62 (54–68)	65 (0–100)
Star-like shape	76 (67–84)	84 (77–89)	78 (70–86)	82 (74–88)	80 (75–85)	68 (58–77)	90 (84–95)	85 (74–91)	79 (70–84)	80 (45–100)
Crescents	85 (77–91)	85 (78–91)	82 (73–89)	88 (81–93)	85 (80–90)	72 (63–80)	92 (86–96)	88 (78–94)	80 (73–86)	83 (52–100)
Predominately oval shape	93 (86–97)	97 (92–99)	95 (89–99)	95 (89–98)	95 (85–100)	93 (86–97)	97 (92–99)	95 (89–99)	95 (89–98)	95 (85–100)
Grooves	100 (95–100)	74 (66–81)	75 (67–81)	100 (96–100)	85 (80–90)	100 (95–100)	82 (75–88)	82 (73–88)	100 (96–100)	90 (74–100)

PPV positive predictive value, *NPV* negative predictive value, *DA* diagnostic accuracy, *CI* confidence interval, *NPs* nuclear protrusions

Table 4 Comparison of NP frequencies between different diagnostic categories

Diagnostic categories	Emerin No. (%positive); *p* value	HE No. (%positive); *p* value
Neoplastic (n: 275) vs. Non- neoplastic (n: 65)	176 (64 %) vs. 2 (3 %); <0.0001	94 (34 %) vs. 0 (0 %); <0.0001
Malignant (n: 198) vs. Benign (n: 142)	158 (80 %) vs. 20 (14 %); <0.0001	84 (42 %) vs. 10 (7 %); <0.0001
FC (n: 48) vs. FA (n: 77)	43 (90 %) vs. 18 (23 %); <0.0001	26 (54 %) vs. 10 (13 %); <0.0001
FV of PTC (n: 98) vs. Non- PTC FN (n: 125)	65 (66 %) vs. 68 (54 %); 0.07	44 (45 %) vs. 43 (34 %); 0.1

NPs nuclear protrusions, *FC* follicualr carcinoma, *FA* follicular adenoma, *PTC* papillary thyroid carcinoma, *FV* follicular variant, *FN* follicualr neoplasia; $p<0.05$ is significant

non- PTC cases was observed [20]. This inconsistency between the results of studies may be related to the difference in the number of cases evaluated and/or the difference in the inclusion criteria used to detect pseudo-inclusions. The diagnostic accuracy rates of this nuclear finding for PTC and FV of PTC was excellent with emerin IHC (DA: 0.91 and 0.90, respectively). This finding is important as in FV of PTC, by HE stain, pseudo- inclusions are infrequent findings [22] as opposed to the usual variant of PTC. Our findings indicate that with emerin IHC the sensitivity and DA of this nuclear alteration for FV of PTC is highly improved, compared to HE (Table 3).

Nuclear grooves in different stages of development could easily be identified with emerin IHC. High sensitivity (100 %) and reasonable specificity (76 %) results of this nuclear feature for PTC was in consistence with the results obtained by using conventional methods in other studies [23–25]. However, in our study, although the sensitivity of grooves detected with HE and emerin IHC was the same (1.00), their diagnostic performance for PTC and FV of PTC was better with HE (Tables 2 and 3). This finding is possibly due to the improvement in the recognition of the more subtle nuclear membrane irregularities that may also be observed in non- PTC lesion.

Predominately oval nuclear shape was observed in 68 % of FV of PTC both with HE and emerin IHC and it was the best performer among all nuclear features examined for FV of PTC diagnosis both with emerin and HE (Table 3). Garlands, crescents and star-like cells also had good diagnostic performances with emerin IHC. These findings were also consistent with the previous study by Kinsella et al. [20].

While, initially, only the previously described nuclear features were the subject of our analysis, we observed that NPs were also easily identified with emerin IHC. These protrusions revealed the same consistency with the main nucleus. They were either, attached to the main nucleus by a stalk (Fig. 2a–c) and appeared as NBs or were observed as small and regularly shaped nuclear fragments in the cytoplasm with no connection to the main nucleus and appeared as MN (Fig. 2d).

Considering the diagnostic criteria that we applied according to the previous literature (Textbox 1), in combination with our findings, we suggest that these nuclear features highlighted with emerin IHC are consistent with micronuclei and nuclear buds which are the known indicators of chromosomal damage [26, 27].

Morphological assessment of several tissue samples including hepatocytes, buccal mucosa cells and cervical cells have been conducted to examine the association of NPs and risk of malignancy. Results of these studies indicate that histopathological or cytological examination of NPs may be used as additional biomarkers in cancer screening [28, 27].

However, although thyroid is an organ that is highly exposed to genotoxic events, studies examining the presence of NPs in tissue samples of thyroid are limited [29–32]

Table 5 Diagnostic accuracy measures of NPs in distinguishing neoplastic lesions from non- neoplastic, malignant form benign, FC from FA and FV of PTC from Non- PTC FN

Diagnostic categories	Emerin, (%) (95 % CI, %)					HE, (%) (95 % CI, %)				
	Sensitivity	Specificity	PPV	NPV	DA	Sensitivity	Specificity	PPV	NPV	DA
Neoplasia	64 (58–69)	97 (88–99)	98 (95–99)	39 (31–46)	70 (44–100)	34 (29–40)	100 (93–100)	100 (95–100)	39 (31–46)	47 (2–100)
Malignancy	79 (73–84)	85 (78–90)	88 (83–92)	75 (68–81)	82 (54–100)	42 (36–49)	93 (87–96)	89 (81–95)	53 (47–60)	63 (12–100)
FC (among non-PTC FN)	89 (77–96)	77 (66–85)	70 (57–81)	92 (82–97)	83 (76–91)	53 (39–67)	87 (77–93)	71 (55–85)	75 (65–84)	74 (23–100)
FV of PTC (among FN)	64 (55–73)	51 (42–59)	50 (42–60)	65 (55–74)	57 (9–100)	44 (35–54)	71 (63–78)	55 (44–66)	62 (53–70)	59 (6–100)

FC follicular carcinoma, *PTC* papillary thyroid carcinoma, *FV* follicular variant, *FN* follicular neoplasia, *CI* confidence interval

Table 6 Diagnostic accuracy measures of TMAs evaluated with HE stain and emerin IHC in distinguishing PTC from non- PTC lesions and FV of PTC from non-PTC FN

Diagnostic accuracy measures	PTC vs. Non-PTC, (%) (95 % CI, %)			FV of PTC vs. non-PTC FN, (%) (95 % CI, %)		
	HE	Emerin	HE and emerin	HE	Emerin	HE and emerin
Sensitivity	70 (63–77)	86 (79–90)	86 (79–90)	55 (46–65)	79 (70–86)	79 (70–86)
Specificity	100 (97–100)	95 (91–97)	100 (97–100)	100 (96–100)	92 (86–96)	100 (96–100)
PPV	100 (95–100)	94 (87–96)	100 (96–100)	100 (91–100)	89 (80–94)	100 (94–100)
NPV	81 (75–85)	89 (84–93)	90 (84–93)	74 (66–80)	85 (77–90)	86 (79–90)
DA	87 (57–100)	91 (73–100)	94 (80–100)	81 (34–100)	86 (62–100)	91 (70–100)

FC follicular carcinoma, *PTC* papillary thyroid carcinoma, *FV* follicular variant, *FN* follicular neoplasia, *CI* confidence interval

MN and NBs are composed of whole chromosomes or chromosomal fragments that are surrounded by a nuclear envelope. Their formation mechanism has not yet been fully clarified. Whether these alterations originate with different mechanisms or they are the different manifestations of the same DNA damage process or both is controversial [26, 27]. However, irrespective of the mechanism, both of these features are known morphological manifestations of chromosomal damage [27]. For this reason, we preferred to evaluate these findings under the same umbrella category of NPs and conducted our statistical analysis accordingly.

To the best of our knowledge, our study is the first in the literature to evaluate the presence of NPs with emerin IHC. The limitation of emerin IHC is that the stain cannot provide the certainty needed to guarantee that these structures are DNA fragments or chromosomes. Nevertheless, the stain highlights that the protrusions originate from the nucleus and are surrounded by nuclear envelope fragments: a finding that is otherwise only suggested by evaluating the regularity of the contours of these formations by conventional or DNA specific stains used in previous studies [27].

Intriguingly, in our study, both with HE and emerin IHC, NPs were more frequent in malignant lesions than benign lesions ($p<0.0001$). This finding takes on added significance, with the observation that NPs are more frequent in FC compared to FA ($p<0.0001$).

NPs could accurately predict malignant behavior in 70 % of the non-PTC FN. Although the positive predictive value of this nuclear feature for malignancy when detected with HE was similar (71 %), sensitivity and diagnostic accuracy with emerin IHC was higher than HE (Table 5) These results led us to the conclusion that NPs detected with emerin IHC may be used as adjunct morphologic biomarkers to evaluate the risk of malignancy in small tissue samples of thyroid, particularly in FN.

Among benign lesions, grooves were more frequent in HT than DH, both with HE and emerin IHC. HT was the only lesion that exhibited NPs (10 %, with emerin IHC), star like shapes (10 %, with emerin IHC) and crescents (14 %, with HE and emerin IHC). The observations above are not surprising as, although conflicting results exist, considerable number of studies indicate that Hashimoto's thyroiditis harbors genetic rearrangements that are associated with papillary thyroid carcinoma [33]. Yet, it would be interesting to know whether detection of NPs, crescents and star like shapes with emerin IHC would serve as an indicator of a pre-neoplastic change, i.e. follicular epithelial dysplasia in HT [34].

Finally, to test if emerin IHC improves the diagnostic efficacy for PTC, we examined the diagnostic accuracy measures of TMAs evaluated with emerin IHC, HE stain and both stains. It has been reported that emerin IHC exhibited a higher sensitivity and specificity for malignancy than HBME-1 and Galectin- 3 [19]. In addition, emerin IHC was found to be increasing the predictive accuracy of HE for PTC [20]. Our results were consistent with the observations of these studies as we noted an improvement in the sensitivity, NPV and DA, both for PTC and FV of PTC (among follicular neoplasia) when both stains were used. This finding suggests that emerin IHC may be used as an adjunct diagnostic tool for PTC. Another observation of this study that may extend the knowledge in this field is that NPs detected with emerin IHC are highly sensitive for malignant behavior and may serve as potential morphological predictors of malignant behavior in small tissue samples. However, more studies are required to translate these observations and suggestions into applications of routine practice.

Acknowledgments This study was presented in part at the annual meeting of the United States and Canadian Academy of Pathology in Baltimore, MD, March 2013.

The authors thank Gulcin Civan for providing their support in immunohistochemical staining.

References

1. Clary KM, Condel JL, Liu Y, Johnson DR, Grzybicki DM, Raab SS (2005) Interobserver variability in the fine needle aspiration biopsy diagnosis of follicular lesions of the thyroid gland. Acta Cytol 49(4): 378–382
2. Elsheikh TM, Asa SL, Chan JK, DeLellis RA, Heffess CS, LiVolsi VA, Wenig BM (2008) Interobserver and intraobserver variation among experts in the diagnosis of thyroid follicular lesions with borderline nuclear features of papillary carcinoma. Am J Clin Pathol 130(5):736–744. doi:10.1309/AJCPKP2QUVN4RCCP
3. Rosai J (2008) Papillary thyroid carcinoma: a root-and-branch re-think. Am J Clin Pathol 130(5):683–686. doi:10.1309/AJCPBF63BWMCYSLW
4. Bussolati G (2008) Proper detection of the nuclear shape: ways and significance. Rom J Morphol Embryol 49(4):435–439
5. Beesley MF, McLaren KM (2002) Cytokeratin 19 and galectin-3 immunohistochemistry in the differential diagnosis of solitary thyroid nodules. Histopathology 41(3):236–243
6. Mai KT, Bokhary R, Yazdi HM, Thomas J, Commons AS (2002) Reduced HBME-1 immunoreactivity of papillary thyroid carcinoma and papillary thyroid carcinoma-related neoplastic lesions with Hurthle cell and/or apocrine-like changes. Histopathology 40(2): 133–142
7. Menon MP, Khan A (2009) Micro-RNAs in thyroid neoplasms: molecular, diagnostic and therapeutic implications. J Clin Pathol 62(11):978–985. doi:10.1136/jcp.2008.063909
8. Nikiforov YE (2002) RET/PTC rearrangement in thyroid tumors. Endocr Pathol 13(1):3–16
9. Nikiforova MN, Biddinger PW, Caudill CM, Kroll TG, Nikiforov YE (2002) PAX8-PPARgamma rearrangement in thyroid tumors: RT-PCR and immunohistochemical analyses. Am J Surg Pathol 26(8):1016–1023
10. Rosai J (2003) Immunohistochemical markers of thyroid tumors: significance and diagnostic applications. Tumori 89(5):517–519
11. Sack MJ, Astengo-Osuna C, Lin BT, Battifora H, LiVolsi VA (1997) HBME-1 immunostaining in thyroid fine-needle aspirations: a useful marker in the diagnosis of carcinoma. Mod Pathol 10(7):668–674
12. Xu XC, el-Naggar AK, Lotan R (1995) Differential expression of galectin-1 and galectin-3 in thyroid tumors. Potential diagnostic implications. Am J Pathol 147(3):815–822
13. Sobrinho-Simoes M, Eloy C, Magalhaes J, Lobo C, Amaro T. Follicular thyroid carcinoma. Mod Pathol 24(Suppl 2):S10–S18. doi:10.1038/modpathol.2010.133
14. Kakudo K, Bai Y, Katayama S, Hirokawa M, Ito Y, Miyauchi A, Kuma K (2009) Classification of follicular cell tumors of the thyroid gland: analysis involving Japanese patients from one institute. Pathol Int 59(6):359–367. doi:10.1111/j.1440-1827.2009.02378.x
15. Holaska JM, Kowalski AK, Wilson KL (2004) Emerin caps the pointed end of actin filaments: evidence for an actin cortical network at the nuclear inner membrane. PLoS Biol 2(9):E231. doi:10.1371/journal.pbio.0020231
16. Wilson KL, Holaska JM, Montes de Oca R, Tifft K, Zastrow M, Segura-Totten M, Mansharamani M, Bengtsson L (2005) Nuclear membrane protein emerin: roles in gene regulation, actin dynamics and human disease. Novartis Found Symp 264:51–58, discussion 58–62, 227–230
17. Fischer AH, Taysavang P, Weber CJ, Wilson KL (2001) Nuclear envelope organization in papillary thyroid carcinoma. Histol Histopathol 16(1):1–14
18. Asioli S, Bussolati G (2009) Emerin immunohistochemistry reveals diagnostic features of nuclear membrane arrangement in thyroid lesions. Histopathology 54(5):571–579. doi:10.1111/j.1365-2559.2009.03259.x
19. Asioli S, Maletta F, Pacchioni D, Lupo R, Bussolati G. Cytological detection of papillary thyroid carcinomas by nuclear membrane decoration with emerin staining. Virchows Arch 457(1):43–51. doi:10.1007/s00428-010-0910-z
20. Kinsella MD, Hinrichs B, Cohen C, Siddiqui MT. Highlighting nuclear membrane staining in thyroid neoplasms with emerin: review and diagnostic utility. Diagn Cytopathol 41(6):497–504. doi:10.1002/dc.22870
21. Rosai J (2011) Thyroid gland. In: Rosai J (ed) Rosai and Ackerman's surgical pathology, 10th edn. Elsevier/Saunders, Philadelphia, PA, p 505
22. Lloyd RV, Erickson LA, Casey MB, Lam KY, Lohse CM, Asa SL, Chan JK, DeLellis RA, Harach HR, Kakudo K, LiVolsi VA, Rosai J, Sebo TJ, Sobrinho-Simoes M, Wenig BM, Lae ME (2004) Observer variation in the diagnosis of follicular variant of papillary thyroid carcinoma. Am J Surg Pathol 28(10):1336–1340
23. Batistatou A, Scopa CD (2009) Pathogenesis and diagnostic significance of nuclear grooves in thyroid and other sites. Int J Surg Pathol 17(2):107–110. doi:10.1177/1066896908316071
24. Rosai J, Kuhn E, Carcangiu ML (2006) Pitfalls in thyroid tumour pathology. Histopathology 49(2):107–120. doi:10.1111/j.1365-2559.2006.02451.x
25. Scopa CD, Melachrinou M, Saradopoulou C, Merino MJ (1993) The significance of the grooved nucleus in thyroid lesions. Mod Pathol 6(6):691–694
26. Fenech M, Kirsch-Volders M, Natarajan AT, Surralles J, Crott JW, Parry J, Norppa H, Eastmond DA, Tucker JD, Thomas P. Molecular mechanisms of micronucleus, nucleoplasmic bridge and nuclear bud formation in mammalian and human cells. Mutagenesis 26(1):125–132. doi:10.1093/mutage/geq052
27. Samanta S, Dey P. Micronucleus and its applications. Diagn Cytopathol 40(1):84–90. doi:10.1002/dc.21592
28. Lee YH, Oh BK, Yoo JE, Yoon SM, Choi J, Kim KS, Park YN (2009) Chromosomal instability, telomere shortening, and inactivation of p21(WAF1/CIP1) in dysplastic nodules of hepatitis B virus-associated multistep hepatocarcinogenesis. Mod Pathol 22(8):1121–1131. doi:10.1038/modpathol.2009.76
29. Caruso RA, Fedele F, Crisafulli C, Paparo D, Parisi A, Luciano R, Cavallari V. Abnormal nuclear structures (micronuclei, nuclear blebs, strings, and pockets) in a case of anaplastic giant cell carcinoma of the thyroid: an immunohistochemical and ultrastructural study. Ultrastruct Pathol 35(1):14–18. doi:10.3109/01913123.2010.517899
30. Nilsson G (1978) Micronuclei studied in fine needle goitre aspirates. Acta Pathol Microbiol Scand A 86(3):201–204
31. Pavlov AV, Aleksandrov Iu K, Beliakov IE, Korableva TV (2007) Morphological analysis of genetically damaged thyrocytes in nodular pathology of the thyroid gland. Vestn Khir Im I I Grek 166(2):58–61
32. Zaharopoulos P, Wong J, Wen JW (1998) Nuclear protrusions in cells from cytologic specimens. Mechanisms of formation. Acta Cytol 42(2):317–329
33. Jankovic B, Le KT, Hershman JM Clinical Review: Hashimoto's thyroiditis and papillary thyroid carcinoma: is there a correlation?. J Clin Endocrinol Metab 98(2):474–482. doi:10.1210/jc.2012-2978
34. Chui MH, Cassol CA, Asa SL, Mete O. Follicular epithelial dysplasia of the thyroid: morphological and immunohistochemical characterization of a putative preneoplastic lesion to papillary thyroid carcinoma in chronic lymphocytic thyroiditis. Virchows Arch 462(5):557–563. doi:10.1007/s00428-013-1397-1